JGR Atmospheres

RESEARCH ARTICLE

10.1029/2023JD039036

Key Points:

- There are high lead-lag correlations of the monthly mean temperatures in the middle and lower reaches of the Yangtze River basin
- The lead-lag relationship between soil temperatures (STs) plays a major role in lead-lag correlation between air temperatures
- The net solar radiation is the main factor affecting the relationships between antecedent and current STs

Supporting Information:

Supporting Information may be found in the online version of this article.

Correspondence to:

Y. Song,
songym@nuist.edu.cn

Citation:

Song, Y., Chen, H., Wang, L., Huang, A., Gu, W., & Ma, Y. (2023). Soil temperature controls the month-to-month lead-lag correlations of near-surface air temperatures in the middle and lower reaches of the Yangtze River basin. *Journal of Geophysical Research: Atmospheres*, *128*, e2023JD039036. https://doi.org/10.1029/2023JD039036

Received 9 APR 2023
Accepted 13 NOV 2023

Author Contributions:

Formal analysis: Haishan Chen
Funding acquisition: Haishan Chen, Anning Huang
Project Administration: Haishan Chen, Anning Huang
Resources: Haishan Chen
Supervision: Haishan Chen, Anning Huang
Visualization: Haishan Chen, Anning Huang, Yutong Ma
Writing – review & editing: Lin Wang, Wei Gu

Soil Temperature Controls the Month-To-Month Lead-Lag Correlations of Near-Surface Air Temperatures in the Middle and Lower Reaches of the Yangtze River Basin

Yaoming Song[1,2], Haishan Chen[1,2], Lin Wang[1,3], Anning Huang[4], Wei Gu[5], and Yutong Ma[2]

[1]Collaborative Innovation Center on Forecast and Evaluation of Meteorological Disasters/Key Laboratory of Meteorological Disaster, Ministry of Education, Nanjing University of Information Science and Technology, Nanjing, China, [2]School of Atmospheric Sciences, Nanjing University of Information Science and Technology, Nanjing, China, [3]Center for Monsoon System Research, Institute of Atmospheric Physics, Chinese Academy of Sciences, Beijing, China, [4]School of Atmospheric Sciences, Nanjing University, Nanjing, China, [5]Laboratory for Climate Studies, National Climate Center, China Meteorological Administration, Beijing, China

Abstract The relationships between the variables at different times are crucial in climate prediction. This study explores the lead-lag correlations between monthly near-surface air temperatures, and analyzes the associated influencing factors and processes using mathematical physics equations and statistical methods, based on monthly observations and ERA5 reanalysis data spanning from 1979 to 2013. The results reveal high lead-lag correlations of near-surface air temperatures in the middle and lower reaches of the Yangtze River basin, characterized by high frequency and intensity of heatwaves. The lead-lag correlations between near-surface temperatures are mainly due to the lead-lag relationships between soil temperatures (STs). Current and accumulated net solar radiation, current latent heat flux and antecedent ST of several or many months ago are the main factors affecting the lead-lag relationships between STs. The processes associated with lead-lag correlations between STs are triggered by antecedent ST, concurrent and accumulated influence factors, respectively. The anomalies of antecedent ST can lead to the anomalies of current one by the persistence of anomaly signals in soil. The effects of accumulated or concurrent influential variables on the lead-lag correlations between STs are attributed to the signals similar to antecedent STs in these influential variables, and the signals may arise from the response of atmosphere to land or ocean forcing. Moreover, the use of reanalysis data increases the uncertainty of the results. The study reveals influential factors and possible physical processes associated with lead-lag correlations between near-surface temperatures, which is helpful for understanding lead-lag relationship between land surface and the atmosphere.

Plain Language Summary Climate prediction depends on the finding of the relationships between the variables at different times. Our studies demonstrate the persistence of substantial lead-lag correlations between the monthly mean near-surface air temperatures in the middle and lower reaches of the Yangtze River basin. Within these lead-lag correlations, the relationship between soil temperatures (STs) at different time leads and lags play a crucial role. Net solar radiation, latent heat flux and antecedent ST of several or many months ago are the main factors affecting the lead-lag relationships between STs. The processes associated with the lead-lag correlations between STs are triggered by antecedent ST, concurrent and accumulated radiation and heat fluxes, respectively. At the monthly, seasonal and longer time scales, the relationships between air temperature or precipitation at different times generally depend on sea surface temperature, soil moisture, ST etc. due to their longer memory relative to atmospheric variables. The lead-lag relationship between variables is the essence of climate prediction, and this study proposes a new idea to analyze the main influencing factors and corresponding physical processes related to the lead-lag relationships between variables in the climate system, which is helpful to understand complex interactions in the climate system.

1. Introduction

The middle and lower Yangtze River basin (MLYRB) is a significant economic and industrial region in China (Y. Zong & Chen, 2000). With its developed economic activities, high population density, and rapid urbanization, the region is particularly vulnerable to frequent meteorological disasters such as drought, flood and heatwaves (He et al., 2001; Nan & Li, 2003; Wang & Xu, 1997; Xie et al., 2020; Y. Zong & Chen, 2000; H. F. Zong et al., 2012). Air temperature, as an important factor in climate system, holds immense importance for society and economy is

10.1029/2023JD039036

particularly important. In the context of global warming, the occurrence of high-temperature events is on the rise (Alexander et al., 2006; IPCC, 2012). Notably, Fang et al. (2017) revealed a close association between extreme air temperatures and the annual average, underscoring the critical need to enhance the accuracy of air temperature prediction in this context.

Land surface is an important part of climate system, and plays a key role in climate variations. Compared to the atmosphere, variable anomalies in the initial field can persist longer in the land surface and the ocean due to the chaotic nature of the atmosphere (Lorenz, 1969; Mariotti et al., 2018), which determines the crucial role of the land surface and the ocean in climate predictions on monthly and longer timescales. Soil temperature (ST) is a key variable in land-atmosphere interactions. Previous studies have shown that the anomalies in spring soil moisture and ST in the lower and middle reaches of the Yangtze River valley can persist into summer and affect the East Asia summer monsoon by changing surface temperature, thereby influencing precipitation in summer (Zhan & Lin, 2011; Zhou, Zuo, & Rong, 2020, Zhou, Zuo, Rong, & Wen, 2020). Moreover, land-atmosphere coupling plays an important role in the improvement of subseasonal prediction skill for heatwaves over the Yangtze River basin (Xie et al., 2020). The above studies mainly focus on the effect of spring soil moisture or ST on summer precipitation or temperature in the Yangtze River basin, and the land processes related to ST or soil moisture are very critical, but lack in-depth analysis.

The essence of climate prediction is to predict the future situation by using the current situation; therefore, finding the relationships between the variables in the present and the variables in the future is crucial. Because of the long memory of ST (Song et al., 2022b; Yang & Zhang, 2016) and the high consistency between ST and surface air temperature at the same time (Zhou, Zuo, & Rong, 2020, Zhou, Zuo, Rong, & Wen, 2020), there may be an obvious connection between surface temperatures at different time lags due to the persistence of ST anomalies. There have been some studies on the persistence of surface air temperatures, that is, the lag correlations between air temperatures. Previous studies showed that long memory in temperature is present and cannot be neglected (Gil-Alaña et al., 2022; Lenti & Gil-Alana, 2021; Li et al., 2021), temperature itself is a skillful predictor of the temperatures 1 month ahead (Kolstad et al., 2015), and persistence forecasts can aid in the subseasonal-to-seasonal prediction of temperatures (Kolstad et al., 2017; Leasor et al., 2019). However, the understanding and research on the lead-lag correlations between near-surface air temperatures remain very limited (Kolstad et al., 2017; Li et al., 2021; Lin et al., 2022; Rypdal et al., 2013). In order to promote deep understanding of the lead-lag relationships between near-surface temperatures, the corresponding influencing factors and physical mechanisms in the MLYRB, the following two questions need to be addressed: (a) what are the characteristics of the lead-lag correlations between near-surface air temperatures in the MLYRB? (b) What are the influential factors and physical processes related to the lead-lag correlations between near-surface air temperatures? The answers to the above questions can deepen the understanding of the land-atmosphere interactions, and provide reference for near-surface temperature predictions.

2. Data and Methods

2.1. Observational and Reanalysis Data

The observational data, provided by the China Meteorological Administration, spans from 1979 to 2013. The observational data includes monthly precipitation, near-surface air temperature (1.5 m) and STs at the soil depths of 5 cm, 10 cm, 20 cm, 40 cm, 80 cm, 160 and 320 cm. Due to the large number of missing values in the observational ST data, the data at 28 sites in the MLYRB (110°–122°E, 27°N–33.5°N) were used for analysis (Figure 2). Additionally, ERA5 reanalysis data spanning from 1979 to 2013 was also utilized, and the variables include monthly and daily sensible heat flux, latent heat flux, reflected solar radiation (SR), upward thermal radiation, net thermal radiation, net SR from land surface and cloud area fraction, in addition to wind velocity, air temperature and geopotential height at 975 hPa and 1,000 hPa. The horizontal resolution of reanalysis data is 0.25° in latitude and longitude. ERA5 monthly near-surface air temperature and ST have very high consistency with the monthly observational data in terms of interannual variations (Figure S1 in Supporting Information S1).

2.2. Methods

The method of analyzing the lead-lag correlations between near-surface air temperatures, and investigating associated influential factors is shown in Figure 1. The −36~36 month lag correlation coefficients for near-surface air

10.1029/2023JD039036

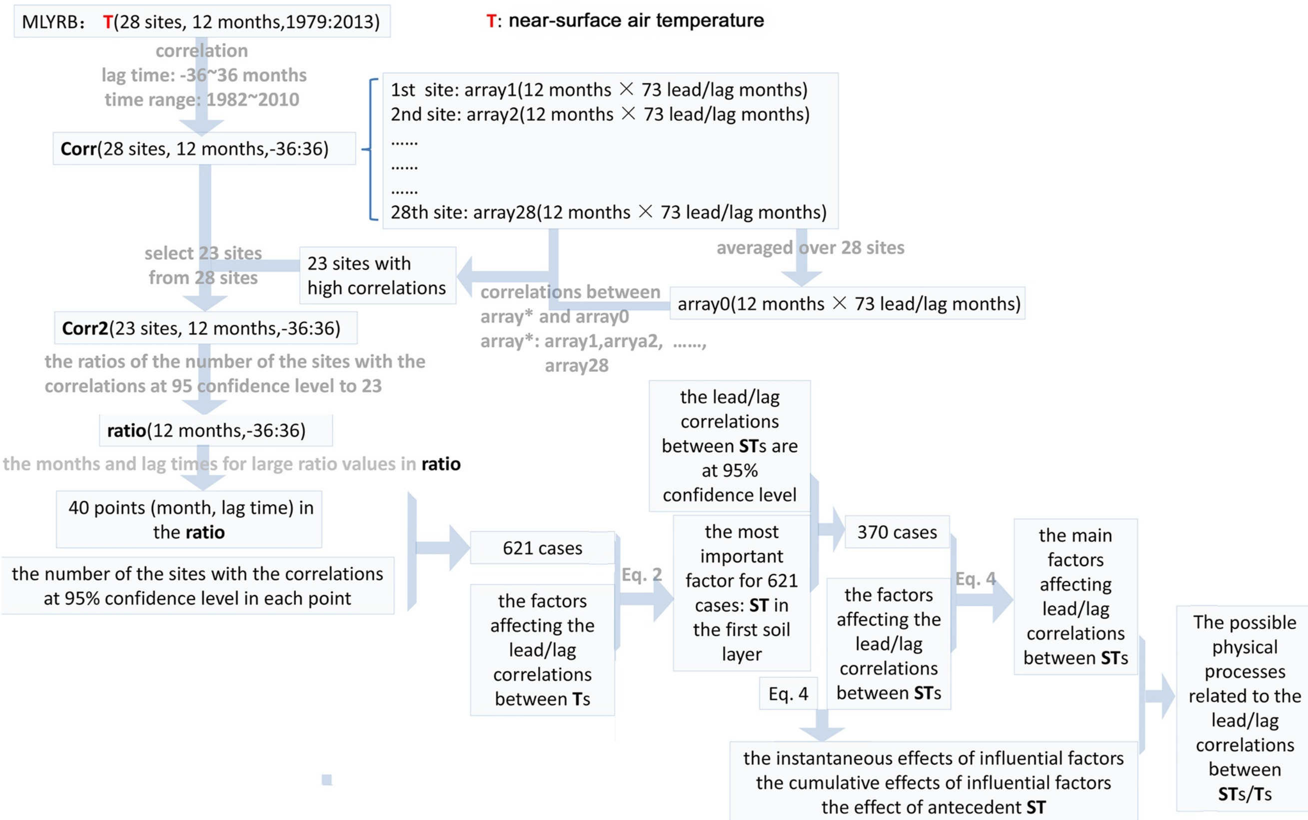

Figure 1. Flowchart of analyzing the lead-lag correlations between near-surface air temperatures, and investigating the associated influential factors.

temperatures during January to December were calculated by the Pearson correlation coefficients. The authors' preliminary study shows these correlation coefficients exhibit similar variations with the change of lag time and month at most sites; thus the characteristics of the correlation coefficients at the above sites can represent the ones in the MLYRB to a great extent. In order to deeply analyze the factors affecting the near-surface air temperature correlations, some cases were selected from 12 months of a year and −36~36 lag months, and there are more sites with correlation coefficients at 95% confidence level in these cases. In order to determine the factors affecting the near-surface temperature correlations, two contribution analysis equations of the correlation coefficients (CAECC) (Equations 12 and 18) were used, which are derived from fluid thermodynamics equation (Equation 1) (Holton, 2004) and the heat budget equation of the first layer of soil (Equation 13) (Oleson et al., 2013), and the two methods correspond to near-surface air temperature and ST in the first layer of soil, respectively. Finally, we analyzed the possible physical processes by which the identified key factors affect the lead-lag correlations between near-surface air temperatures using observational and reanalysis data.

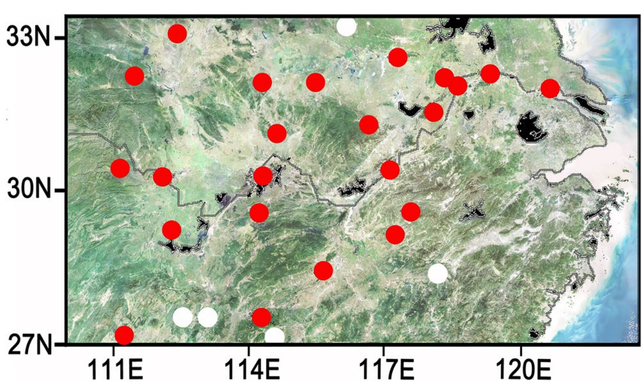

Figure 2. The locations of the 28 sites (white and red solid dots) with few observed missing data in the middle and lower Yangtze River basin. The lead-lag correlation coefficients of near-surface temperatures at any site (red dot) are basically consistent with the ones at other sites (red dots) with the change of month and lag time.

The derivation of CAECC for near-surface air temperature and ST in the first layer of soil is outlined next.

Air temperature is calculated by Equation 1 (Holton, 2004).

$$\frac{\partial T}{\partial t} = -\vec{V}_h \cdot \nabla_h T - \omega \frac{\partial T}{\partial p} + \frac{RT}{c_p p}\omega + \frac{Q_{\mathrm{derivative}}}{c_p} \tag{1}$$

Here T is air temperature. The first and second terms on the right side of Equation 1 are horizontal and vertical advection of temperature, respectively. $\vec{V}_h$ and ω are the horizontal and vertical velocities in the pressure coordinate, respectively. $Q_{\mathrm{derivative}}$ represents diabatic heating, such as heat and radiation fluxes. p, c_p are air pressure and dry air specific gas constant, respectively. The integration of both sides of Equation 1 over time gives Equation 2. Equation 2 is discretized using the finite difference method to obtain Equation 3. Expand the terms of Equation 3 to get Equation 4.

$$T_m = \int_n^m \left(-\vec{V}_h \cdot \nabla_h T - \omega \frac{\partial T}{\partial p} + \frac{RT}{c_p p}\omega + \frac{Q_{\text{derivative}}}{c_p} \right) dt + T_n \tag{2}$$

$$T_m = \sum_{i=n}^{m} \left(-\vec{V}_h \cdot \nabla_h T - \omega \frac{\partial T}{\partial p} + \frac{RT}{c_p p}\omega + \frac{Q_{\text{derivative}}}{c_p} \right)_i \Delta t + T_n \tag{3}$$

$$\begin{aligned} T_m = & \left[\left(-\vec{V} \cdot \nabla_h T \right)_n + \left(-\vec{V} \cdot \nabla_h T \right)_{n+1} + \cdots\cdots + \left(-\vec{V} \cdot \nabla_h T \right)_m \right] \Delta t + \\ & \left[\left(-\omega \frac{\partial T}{\partial p} + \frac{RT}{c_p p}\omega + \frac{Q_{\text{derivative}}}{c_p} \right)_n + \left(-\omega \frac{\partial T}{\partial p} + \frac{RT}{c_p p}\omega + \frac{Q_{\text{derivative}}}{c_p} \right)_{n+1} + \cdots\cdots + \right. \\ & \left. \left(-\omega \frac{\partial T}{\partial p} + \frac{RT}{c_p p}\omega + \frac{Q_{\text{derivative}}}{c_p} \right)_m \right] \Delta t + T_n \end{aligned} \tag{4}$$

Here m and n represent different times, respectively. Because of the short memory of atmospheric anomalies (Lorenz, 1969), the terms related to atmosphere are removed in Equation 4, and Equation 5 is obtained. The terms in Equation 5 are subtracted climate state to obtain Equation 6. Equation 7 is obtained using the same approach as Equation 6.

$$T_m \approx \left(-\vec{V} \cdot \nabla_h T \right)_m \Delta t + \left(-\omega \frac{\partial T}{\partial p} + \frac{RT}{c_p p}\omega + \frac{Q_{\text{derivative}}}{c_p} \right)_m \Delta t + R_m \tag{5}$$

$$T'_m \approx \left(-\vec{V} \cdot \nabla_h T \right)'_m \Delta t + \left(\frac{Q_{\text{derivative}}}{c_p} \right)'_m \Delta t + \left(-\omega \frac{\partial T}{\partial p} + \frac{RT}{c_p p}\omega \right)'_m \Delta t + R'_m \tag{6}$$

$$T'_n \approx \left(-\vec{V} \cdot \nabla_h T \right)'_n \Delta t + \left(\frac{Q_{\text{derivative}}}{c_p} \right)'_n \Delta t + \left(-\omega \frac{\partial T}{\partial p} + \frac{RT}{c_p p}\omega \right)'_n \Delta t + R'_n \tag{7}$$

In Equations 6 and 7, diabatic heating $Q_{\text{derivative}}$ is related to sensible heat flux (SH), latent heat flux (LH), reflected solar radiation (SR) and upward thermal radiation (LR) from land surface, etc. Since SH, LH, SR, LR are closely related to ST, the expression of $Q_{\text{derivative}}$ is further simplified to obtain Equation 8.

$$Q_{\text{derivative}} = f(\text{SR}, \text{LR}, \text{SH}, \text{LH}) + \text{Res} = g(\text{ST}) + \text{Resi} \approx \alpha\text{ST} + \text{Resid} \tag{8}$$

The linear expressions (Equations 9 and 10) are obtained for Equations 6 and 7 using multiple linear regression method. Resi and Resid are the residual terms.

$$T'_m \approx a\left(-u\frac{\partial T}{\partial x} \right)'_m + b\left(-v\frac{\partial T}{\partial y} \right)'_m + c\left(-\omega\frac{\partial T}{\partial p} \right)'_m + d\left(\frac{\text{RT}}{c_p p}\omega \right)'_m + e(\text{ST})'_m + \text{Re}'_m \tag{9}$$

$$T'_n \approx i\left(-u\frac{\partial T}{\partial x} \right)'_n + j\left(-v\frac{\partial T}{\partial y} \right)'_n + k\left(-\omega\frac{\partial T}{\partial p} \right)'_n + l\left(\frac{\text{RT}}{c_p p}\omega \right)'_n + o(\text{ST})'_n + \text{Re}'_n \tag{10}$$

Here Re is the residual term. Equation 9 multiplied by Equation 10 gives Equation 11, and the covariance terms are included in Resi′.

$$\begin{aligned} T'_m \cdot T'_n = & ai\left(-u\frac{\partial T}{\partial x} \right)'_m \cdot \left(-u\frac{\partial T}{\partial x} \right)'_n + bj\left(-v\frac{\partial T}{\partial y} \right)'_m \cdot \left(-v\frac{\partial T}{\partial y} \right)'_n + ck\left(-\omega\frac{\partial T}{\partial p} \right)'_m \cdot \left(-\omega\frac{\partial T}{\partial p} \right)'_n \\ & + dl\left(\frac{\text{RT}}{c_p p}\omega \right)'_m \cdot \left(\frac{\text{RT}}{c_p p}\omega \right)'_n + eo\text{ST}'_m \cdot \text{ST}'_n + \text{Resi}' \end{aligned} \tag{11}$$

Equation 11 is adjusted to obtain the factors related to the lead-lag correlation coefficient between air temperatures (Equation 12).

$$\begin{aligned}\mathrm{corr}\left(T'_m, T'_n\right) &= T'_m \cdot T'_n / \left(\sqrt{T'_m \cdot T'_m}\sqrt{T'_n \cdot T'_n}\right) \\ &= \left\{ ai\left(-u\frac{\partial T}{\partial x}\right)'_m \cdot \left(-u\frac{\partial T}{\partial x}\right)'_n + bj\left(-v\frac{\partial T}{\partial y}\right)'_m \cdot \left(-v\frac{\partial T}{\partial y}\right)'_n + \right. \\ &\quad ck\left(-\omega\frac{\partial T}{\partial p}\right)'_m \cdot \left(-\omega\frac{\partial T}{\partial p}\right)'_n + dl\left(\frac{\mathrm{RT}}{c_p p}\omega\right)'_m \cdot \left(\frac{\mathrm{RT}}{c_p p}\omega\right)'_n + \\ &\quad \left. eo\mathrm{ST}'_m \cdot \mathrm{ST}'_n + \mathrm{Resi}' \right\} / \left(\sqrt{T'_m \cdot T'_m}\sqrt{T'_n \cdot T'_n}\right)\end{aligned} \tag{12}$$

Soil temperature at 0.05 m soil depth is calculated by Equation 13 (Oleson et al., 2013).

$$\sigma\frac{\partial \mathrm{ST}}{\partial t} = -\mathrm{SH} - \mathrm{LE} - \mathrm{net}T + \mathrm{net}S + \mathrm{Residual} \tag{13}$$

Here ST is soil temperature at 0.05 m, σ is the amount of heat required to warm the soil by one degree Celsius. SH, LE, net$T$ and net$S$ are sensible heat flux, latent heat flux, net thermal radiation and net SR, respectively. Residual represents other impact factors, including the heat transferred from underlying soil, vegetation, snow, etc. Equation 13 is discretized using the finite difference method to obtain Equation 14. m and n represent different times, respectively in Equation 14.

$$\mathrm{ST}_m = \frac{1}{\sigma}\Delta t \sum_{i=n+1}^{m} (\mathrm{SH} + \mathrm{LE} + \mathrm{net}S + \mathrm{net}T + \mathrm{Residuals})_i + ST_n \tag{14}$$

Equation 15 is obtained by rearranging Equation 14, and Residu is related to other factors.

$$\begin{aligned}\mathrm{ST}_m =& \frac{1}{\sigma}\Delta t(\mathrm{SH}_m + \mathrm{LE}_m + \mathrm{net}S_m + \mathrm{net}T_m) + \frac{1}{\sigma}\Delta t \sum_{i=n+1}^{m-1} (\mathrm{SH} + \mathrm{LE} + \mathrm{net}S + \mathrm{net}T)_i + \\ & \mathrm{ST}_n + \mathrm{Residu}\end{aligned} \tag{15}$$

Express the first and second terms on the right side of Equation 15 in the form of implicit functions to get Equation 16. Due to the important effect of precipitation on ST, precipitation is added to the first and second terms on the right side of Equation 16, and Residual is related to the other factors excluding precipitation.

$$\begin{aligned}\mathrm{ST}_m =& F(\mathrm{SH}_m, \mathrm{LE}_m, \mathrm{net}S_m, \mathrm{net}T_m, \mathrm{Rain}_m) + G\left(\sum_{i=n+1}^{m-1}\mathrm{SH}_i, \sum_{i=n+1}^{m-1}\mathrm{LE}_i, \sum_{i=n+1}^{m-1}\mathrm{net}S_i, \sum_{i=n+1}^{m-1}\mathrm{net}T_i, \sum_{i=n+1}^{m-1}\mathrm{Rain}_i\right) \\ & + \mathrm{ST}_n + \mathrm{Residual}\end{aligned} \tag{16}$$

The linear relationship between ST anomaly and other factors can be obtained by multiple linear regression method (Equation 17). The superscript $'$ of a variable represents the anomaly of the variable in Equation 17.

$$\begin{aligned}\mathrm{ST}'_m =& \left(\alpha\mathrm{SH}'_m + \beta\mathrm{LE}'_m + \gamma\mathrm{net}S'_m + \varepsilon\mathrm{net}T'_m + \eta\mathrm{Rain}'_m\right) \\ & + \left(\lambda\sum_{i=n+1}^{m-1}\mathrm{SH}'_i + \delta\sum_{i=n+1}^{m-1}\mathrm{LE}'_i + \mu\sum_{i=n+1}^{m-1}\mathrm{net}S'_i + \upsilon\sum_{i=n+1}^{m-1}\mathrm{net}T'_i + \xi\sum_{i=n+1}^{m-1}\mathrm{Rain}'_i\right) + \kappa\mathrm{ST}'_n + \mathrm{Residual}'\end{aligned} \tag{17}$$

Multiply ST'_n on both sides of Equation 17 and divide Equation 17 by $\sqrt{\mathrm{ST}'_m \cdot \mathrm{ST}'_m}\sqrt{\mathrm{ST}'_n \cdot \mathrm{ST}'_n}$ to obtain the correlation coefficient between STs at m and n moments and the factors affecting the correlation coefficients (Equation 18). The inner products of each terms in Equation 17 with ST'_n represents the projections of each terms on ST'_n.

$$\begin{aligned}\mathrm{corr}\left(\mathrm{ST}'_m, \mathrm{ST}'_n\right) &= \mathrm{ST}'_m \cdot \mathrm{ST}'_n / \left(\sqrt{\mathrm{ST}'_m \cdot \mathrm{ST}'_m}\sqrt{\mathrm{ST}'_n \cdot \mathrm{ST}'_n}\right) \\ &= \left\{\alpha\mathrm{SH}'_m \cdot \mathrm{ST}'_n + \beta\mathrm{LE}'_m \cdot \mathrm{ST}'_n + \gamma\mathrm{net}S'_m \cdot \mathrm{ST}'_n + \varepsilon\mathrm{net}T'_m \cdot \mathrm{ST}'_n + \eta\mathrm{Rain}'_m \cdot \mathrm{ST}'_n \right. \\ &\quad + \left(\lambda\sum_{i=n+1}^{m-1}\mathrm{SH}'_i\right) \cdot \mathrm{ST}'_n + \left(\delta\sum_{i=n+1}^{m-1}\mathrm{LE}'_i\right) \cdot \mathrm{ST}'_n + \left(\mu\sum_{i=n+1}^{m-1}\mathrm{net}S'_i\right) \cdot \mathrm{ST}'_n + \left(\upsilon\sum_{i=n+1}^{m-1}\mathrm{net}T'_i\right) \cdot \mathrm{ST}'_n \\ &\quad \left. + \left(\eta\sum_{i=n+1}^{m-1}\mathrm{Rain}'_i\right) \cdot \mathrm{ST}'_n + \kappa\mathrm{ST}'_n \cdot \mathrm{ST}'_n + Resid' \right\} / \left(\sqrt{\mathrm{ST}'_m \cdot \mathrm{ST}'_m}\sqrt{\mathrm{ST}'_n \cdot \mathrm{ST}'_n}\right)\end{aligned} \tag{18}$$

10.1029/2023JD039036

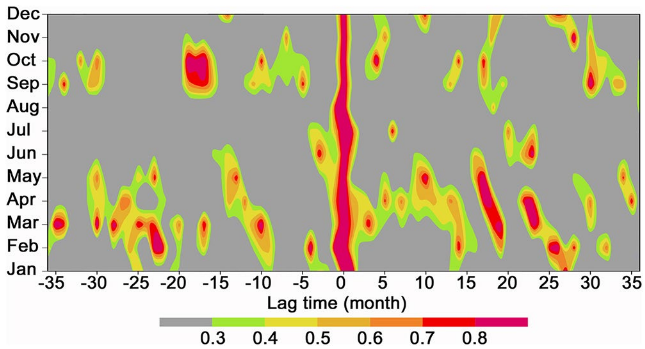

Figure 3. The ratios of the number of the sites where the lead-lag correlation coefficients between near-surface temperatures are at the 95% confidence level to the number of the sites with red dot shown in Figure 2.

Where corr is the correlation coefficient; apostrophe denotes the anomaly from the climate mean; u, v are the longitudinal, latitudinal velocities in the pressure coordinate, respectively; Resi and Resid are the residual terms; the coefficients like a, b and α are regression coefficients; Residual denotes the others. In Equation 18, the first five terms on the right side are the instantaneous effects of various variables, the sixth to tenth terms are the cumulative effects of various variables, and the eleventh term corresponds to the effect of ST of n times.

3. Results

In the MLYRB, the lead-lag correlation coefficients between near-surface temperatures at most sites shows similar variations with the change of lag time and month (Figure S2 in Supporting Information S1), and the number of the sites is 23 (with red dot in Figure 2). The ratios of the number of the sites where the correlation coefficients are at the 95% confidence level to the number of the sites with red dot are shown in Figure 3 for the −36∼36 lag months during January to December. As shown in Figure 3, near-surface temperature exhibits significant lead-lag correlations from −36 to 36 months at more sites in February, March April, September and October than in January, July, August and December. So the question is joined: what affect these lead-lag correlations between near-surface air temperatures?

Based on the information in Figure 3, some cases are selected for the in-depth analysis of the influential factors and possible physical processes affecting the lead-lag correlations between near-surface temperatures (Figure S3 in Supporting Information S1). These cases correspond to the lead-lag correlations with 95% confidence level between near-surface temperatures at the 23 sites for the large ratios at −36∼36 lag months and 12 months of a year in Figure 3, and the number of these cases is 621. Using the CAECC, the ST in the first soil layer plays a major role in the lead-lag correlations between near-surface temperatures, and the contribution of ST averaged over all cases is 59.60% (Figure 4). The effects of temperature advection and the work done on the environment through air expansion are not important (Figure 4). From Equation 12, the lead-lag relationships between STs contribute to the lead-lag correlations between near-surface temperatures at corresponding times by land-atmosphere interactions. Using the CAECC, the analysis of 370 cases show that the factors affecting the lead-lag correlations between STs are in order of importance: current net SR, accumulated net SR, current latent heat flux, antecedent ST of several or many months ago, current latent heat flux and others (Figure 5). The following three questions are

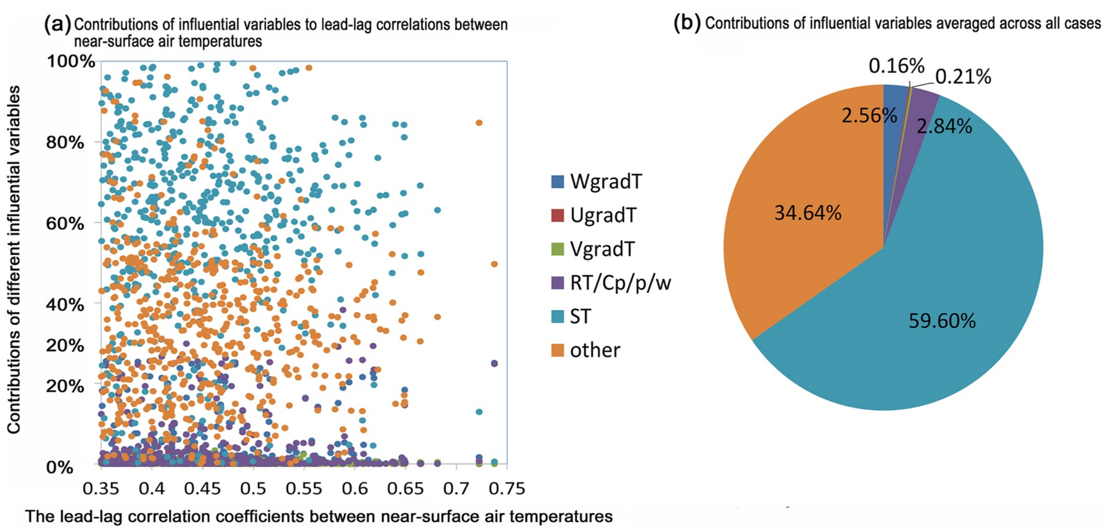

Figure 4. The contributions of latitudinal, longitudinal and vertical advection of air temperature (UgradT, VgradT, WgradT), work done on the environment through air expansion (RT/Cp/p/w), soil temperature at 0.05 m soil depth and other factors to the lead-lag correlations between near-surface temperatures for the 621 cases. Panel (a) shows the contributions of six influential factors to the lead-lag correlations for all cases, and each dot represents the contribution of a particular influential factor in a case. Panel (b) shows the average of the contributions of these six influential factors across all cases.

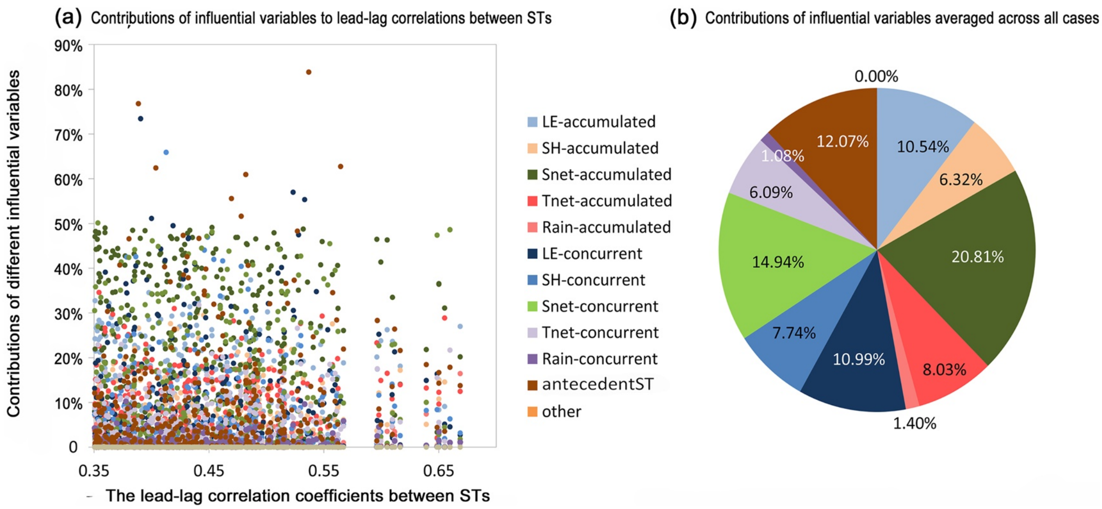

Figure 5. The contributions of accumulated/current sensible (SH-accumulated/SH-current) accumulated/current latent heat fluxes (LE-accumulated/LE-current), accumulated/current net solar radiation (Snet-accumulated/Snet-current), accumulated/current net thermal radiation from land surface (Tnet-accumulated/Tnet-current), accumulated/current rain (Rain-accumulated/Rain-current), and the soil temperature (ST) of several or many months ago (antecedentST) to the lead-lag correlations of STs at 0.05 m soil depth for the 370 cases. Panel (a) shows the contributions of 12 influential factors to the lead-lag correlations for all cases, and each dot represents the contribution of a particular influential factor in a case. Panel (b) shows the average of the contributions of these 12 influential factors across all cases.

raised: What are the characteristics of these factors affecting the lead-lag correlations between STs? What affects net SR which plays an important role in ST lead-lag correlations? And what are the possible processes related to ST lead-lag correlations?

Similar to Figure 5b, Figure 6 shows current net SR, accumulated net SR, current latent heat flux and antecedent ST of several or many months ago are the main factors affecting the lead-lag correlations between STs. The ratios for current net SR, accumulated net SR, current latent heat flux and antecedent ST averaged over all lag times are 13.9%, 11.2%, 3.8% and 3.9%, respectively (Figure 6b). The ratios for current net SR, accumulated net SR, current latent heat flux and antecedent ST averaged over 12 months of a year are 33.8%, 26.3%, 7.2%, and 14.2%, respectively (Figure 6d). The effects of the most factors are approximately evenly distributed in −36~36 lag months, and there are no obvious concentrations at some certain lead-lag times (Figure 6a). The effects of current sensible heat flux are mainly concentrated in the relationships between current STs and the ones in the previous month (Figure 6a). For the lead-lag correlations between STs, the effects from current latent heat flux are more important in the first half of the year than in the second half, while antecedent ST has more important effect in winter than in other seasons (Figure 6c). Additionally, net SR always plays an important role in the lead-lag correlations between STs throughout 12 months (Figure 6c).

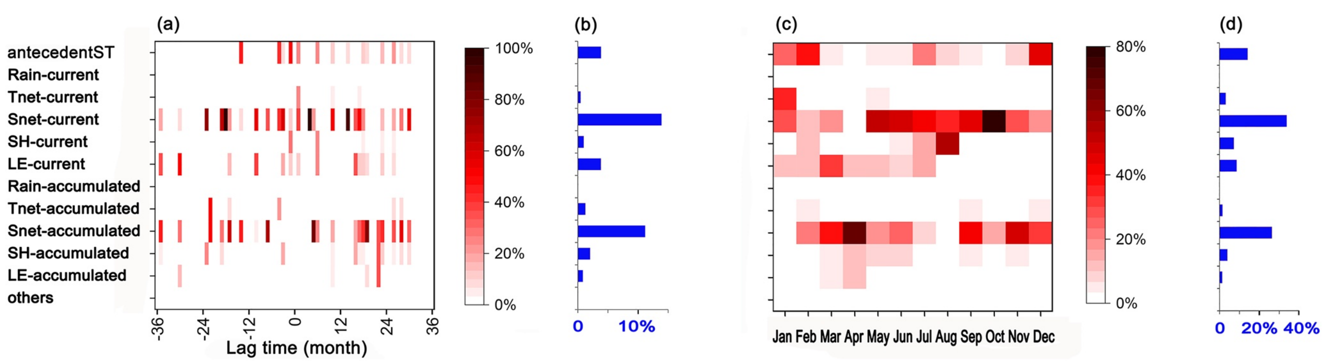

Figure 6. The ratios of the number of the cases in which a certain influential variable contributes the most to the lead-lag correlations between soil temperatures (STs) to the number of all cases. In all the cases, both the lead-lag correlations between near-surface temperatures and the lead-lag correlations between STs are at 95% confidence level at a certain lag time (a, b) or in a certain month (c, d). The ratios for −36~36 lag months and 12 months of a year are shown in (a) and (c), respectively. The ratios averaged over all lag times and averaged over 12 months of a year are shown in (b) and (d), respectively.

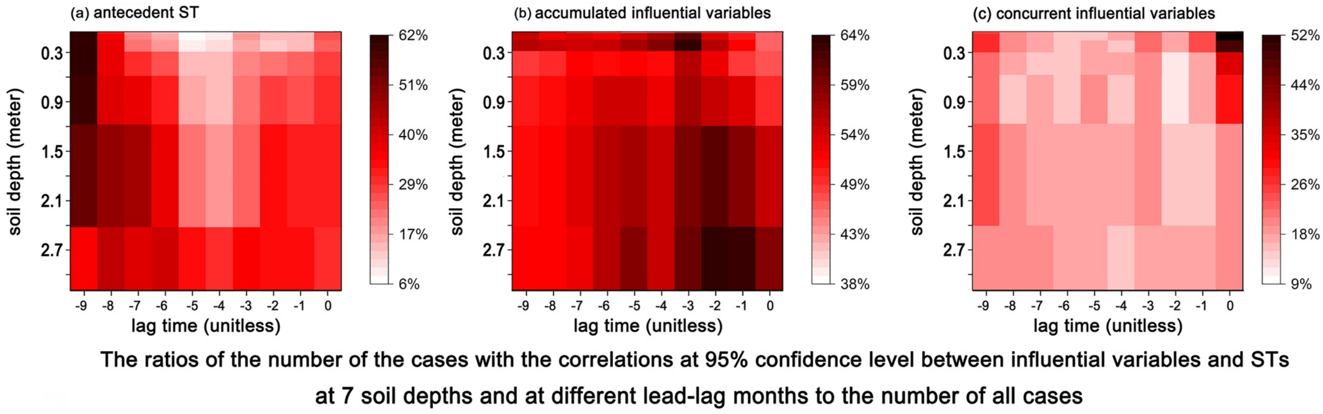

Figure 7. The ratios of the cases with the correlations at the 95% confidence level between the influential factors and soil temperatures (STs) in seven soil layers at different lag times to all cases. The influential factors include antecedent ST (a), accumulated influential variables (b), and concurrent influential variables (c). In these three panels, the lag times correspond to the projections of the true lead-lag times onto these 10 times.

Generally, cloud cover determines the SR reaching the land surface. Based on ERA5 reanalysis data, the correlation coefficient averaged over 621 cases between total cloud cover and the net SR is −0.85 (Figure S4 in Supporting Information S1) in the MLYRB, which further confirms the effect of cloud cover on the net SR in the MLYRB. Combined with Figure 5, no matter the cloud cover from the antecedent to current time, or the current cloud cover, both play a key role in the lead-lag correlations between current and antecedent STs in the MLYRB.

$$\begin{aligned} \mathrm{ST}_m = {} & \frac{\Delta t}{\sigma}(\mathrm{SH}_m + \mathrm{LE}_m + \mathrm{net}S_m + \mathrm{net}T_m + \mathrm{Rain}_m) \\ & + \frac{\Delta t}{\sigma}\left(\sum_{i=n+1}^{m-1}\mathrm{SH}_i + \sum_{i=n+1}^{m-1}\mathrm{LE}_i + \sum_{i=n+1}^{\mathrm{m}-1}\mathrm{net}S_i + \sum_{i=n+1}^{m-1}\mathrm{net}T_i\right) + \mathrm{ST}_n \end{aligned} \tag{19}$$

Here the meanings of the variables, subscripts and superscripts in Equation 19 are as described in Equations 13 and 18. The first and second terms on the right side of Equation 19 are concurrent and accumulated effects of influential variables, respectively. And the third term on the right side is the effect from antecedent ST. In the second terms on the right side, the summation ranges from the time of antecedent ST to the month preceding the current ST time, which are also the accumulated ranges of influential variables in this paper.

From Equation 19, which is the finite-difference form of Equation 13, the anomalies of antecedent ST can lead to the anomalies of current ST, while the accumulated and current heat and radiation fluxes can change the effect of antecedent ST on current ST by adding additional signals in the persistence of antecedent ST anomaly signals. The effects of the influential variables on the lead-lag correlations between STs depend on their influence on ST and the signals similar to antecedent ST in these influential variables. In order to study the roles of antecedent ST, accumulated and concurrent influential variables in the correlations between antecedent ST and current one, we analyzed the cases in which the contributions of the influential variables to the lead-lag correlations between STs are bigger than 0.2 in Figure 5a. Moreover, the strength with which the influential variables affect STs in 7 soil layers and at different lead-lag times is represented by the ratios of the number of the cases in which the correlations between the influential variables and current ST are at 95% confidence level to the number of all cases (Figure 7).

Based on Figure 7 and Equation 19, the possible processes of antecedent ST, concurrent and accumulated influential variables affecting the lead-lag correlations of STs can be deduced. Figure 7a shows that the anomalies of antecedent ST can persist in the first layer of soil, and then affect current ST in the first layer of soil. Moreover, the anomalies of antecedent ST can propagate downwards, mainly persist in the fourth to seventh layers of soil, propagate upwards in soil under suitable conditions, and then affect current ST in the first layer of soil (Figure 7a). However, the effect of antecedent ST on current ST changes with the addition of the signals from concurrent and accumulated influential variables, thus the effect of antecedent ST are negligible in some cases. Figure 7b shows that the effects of accumulated variables on ST propagate downward with time and can also persist in the first layer of soil, and then affect the ST in the first layer of soil. The effects of concurrent influential variables on ST are mainly concentrated in the middle and upper soil layers at the same time (Figure 7c). In Figures 7b and 7c, the high correlations between concurrent or accumulated influential variables and antecedent ST are

Journal of Geophysical Research: Atmospheres 10.1029/2023JD039036

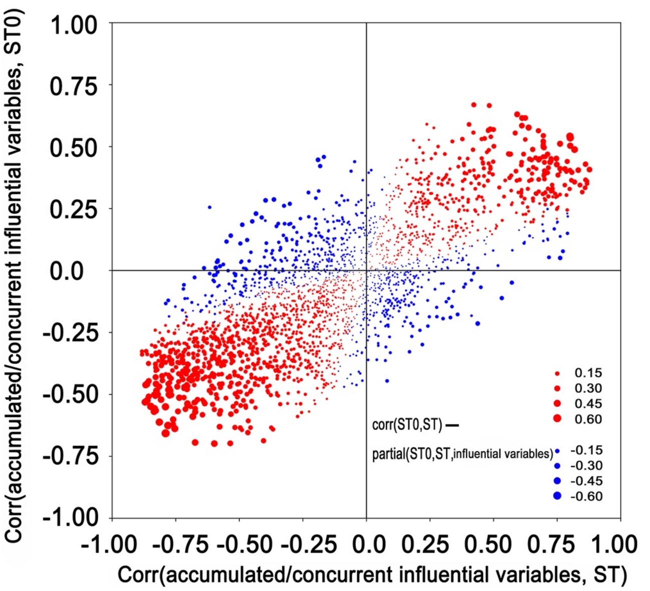

Figure 8. The relationships among the correlations between accumulated/concurrent variables and current soil temperatures (STs), the correlations between accumulated/concurrent variables and antecedent ST, and the differences in the correlation coefficients between antecedent and current STs with and without the signals from concurrent and accumulated variables. ST0, ST represent antecedent and current STs at 0.05 m soil depth, respectively. Corr (A, B) denotes the correlation coefficients between A and B, and partial (A, B, C) is the correlation coefficients between A and B that remains once the linear influences of C have been eliminated.

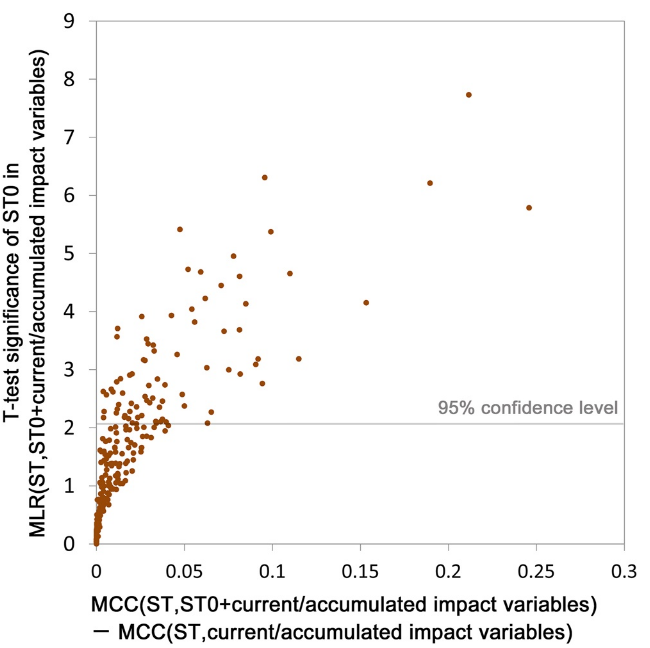

Figure 9. The abscissa is the differences of the multiple correlation coefficients (MCC) between current soil temperature (ST) and all influential factors with and without removing antecedent ST. The ordinate is the statistical significance of antecedent ST in the regression equations of current ST on all influential variables. MCC (A, B) represents the MCC between A and B.

attributed to the common signals in the influential variables and antecedent STs, and these common signals may also help enhance the correlations between antecedent ST and current ones. For example, though current net SR can only affect current ST, there are still statistically significant correlations between antecedent ST and current net SR due to the common signals in them, and these common signals may come from the net solar radiations at the antecedent and current times, respectively, which results in the high correlations between antecedent and current ST. In other words, the concurrent net solar radiations in the antecedent and current times lead to the anomalies of STs at the corresponding times, respectively, and the common signals in net solar radiations in the two times cause the high lead-lag correlations between STs (Figure 10).

As mentioned above, the physical processes by which concurrent and accumulated influential variables affect the lead-lag correlations between STs may be related to the signals similar to antecedent and current ST contained in the influential variables. In order to better understand the processes associated to concurrent and accumulated variables affecting the correlations between antecedent ST and current ST, the differences of the correlation coefficients with and without the signals from concurrent and accumulated variables are analyzed. Figure 8 shows that the effects of concurrent and accumulated influential variables on the relationships between current and antecedent STs are very important. When the correlation coefficients between the influential variables and antecedent ST have the same sign as the ones between the influential variables and current ST, the correlations between antecedent and current ST are obviously weaker after the signals from the influential variables are removed, while the correlations between antecedent and current STs become stronger in the opposite conditions (Figure 8), which is because of the positive correlations between current and antecedent STs. Moreover, the larger absolute values of the correlation coefficients between influential variables and antecedent or current ST mean the greater effects of the influential variables on the correlations between antecedent ST and current one (Figure 8). In other words, whether the concurrent and accumulated influential variables strengthens or weakens the relationships between antecedent and current STs depends on whether the correlation coefficients between influential variables and antecedent ST and the correlation coefficients between influential variables and current ST are of the same sign.

In the cases where the effects from concurrent and accumulated influential variables are negligible, antecedent ST determines the lead-lag correlations between STs. The variances of current ST explained by antecedent ST, concurrent and accumulated influential variables are larger than those explained by only concurrent and accumulated variables, and the differences in the corresponding multiple correlation coefficients are shown in Figure 9. Moreover, the statistical significances of antecedent ST in the regression equations of current ST on antecedent ST, concurrent and accumulated variables are analyzed by Student's test. On the whole, as the statistical significance of antecedent ST in the regression equations increases, the contribution of antecedent ST to the variations of current ST increases (Figure 9). It can be concluded that antecedent ST is a necessary part of current ST, and plays an important role in the lead-lag correlations between STs in some cases.

Generally speaking, concurrent and accumulated influential variables all have important effects on the lead-lag correlations between STs (Figures 7–9, Equations 18 and 19). The anomalies of antecedent ST persist in soil and then affect current ST, which can lead to the lead-lag correlations between STs.

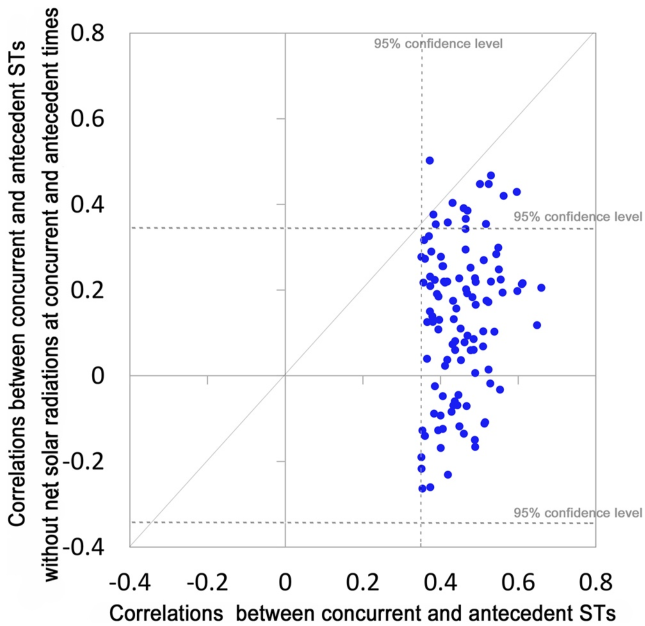

Figure 10. The differences of the correlation coefficients between current and antecedent soil temperatures with and without removing current and antecedent net solar radiations.

Moreover, the concurrent and accumulated variables with the signals similar to antecedent ST can affect the lead-lag correlations between STs, because both accumulated and concurrent variables can affect current ST by anomaly signal persistence and concurrent land-atmosphere interactions. The existence of the signals similar to antecedent ST in current influential variables may be due to the high correlations between antecedent atmospheric forcing signals and current ones, For example, as the most important influencing factor (Figure 5b), both net SR in antecedent and current times contain the signals similar to antecedent ST, which leads to the high correlations between antecedent ST and current one (Figure 10).

4. Conclusions and Discussions

There are high −36~36 month lag correlations between the monthly mean near-surface temperatures at the height of 1.5 m in the MLYRB, characterized by high frequency and intensity of heatwaves (Figure S5 in Supporting Information S1). These high correlations are mainly in February, March, April, September and October for the most sites in the MLYRB. Based on the fluid thermodynamics equation (Equation 1) and the CAECC, it can be concluded that the lead-lag relationship between STs plays a major role in the lead-lag correlations between near-surface temperatures through land-atmosphere interactions, and the contribution of ST averaged over all cases is 59.60% (Figure 4, Equation 12). The studies of Kolstad et al. (2017) also confirmed the important role of ST in the lag relationships between near-surface temperatures. Furthermore, the relationships between antecedent and current STs depend on current net SR, accumulated net SR, current latent heat flux, antecedent ST and other factors. Net SR is the most important influencing factor in the lead-lag correlations between STs.

The signals similar to antecedent ST contained in current ST cause the lead-lag correlations between STs, and these signals come from three sources which are antecedent ST, concurrent and accumulated influential variables. The associated physical processes are shown in Figure 11, which is based on Figure 7. As shown in Equation 19 and Figure 7a, the anomalies of antecedent ST can lead to the anomalies of current ST by the persistence of anomaly signals in soil, which implies the correlations between antecedent and current STs. The anomalies of antecedent ST can persist in the shallow soil, and then affect current ST in the shallow soil (Song et al., 2022a, 2022b). Moreover, the anomalies of antecedent ST can propagate downwards, mainly persist in the middle and deep soil, propagate upwards in soil under suitable conditions (Matsumura & Yamazaki, 2012; Schaefer et al., 2007; Song et al., 2022a, 2022b), and then affect current ST in the shallow soil (Figure 7a). Both processes can also be deduced based on the studies of Kolstad et al. (2017). In the persistence of anomaly signals from antecedent

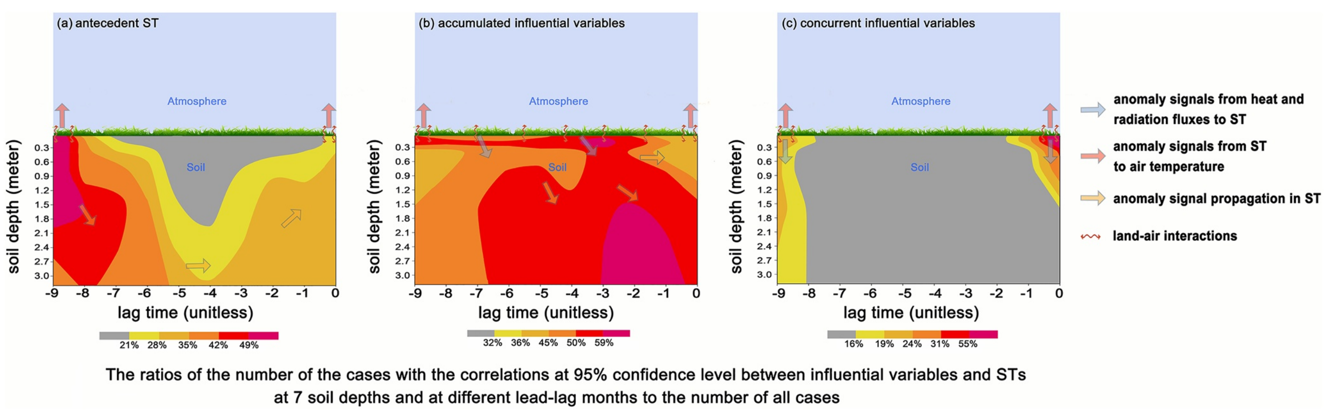

Figure 11. Concept map for the physical processes associated with the lead-lag correlations between near-surface temperatures, and the processes are related to antecedent (a) soil temperature, (b) accumulated variables, and (c) concurrent variables, respectively.

ST, the effects of antecedent ST on current one change with the addition of the signals from accumulated variables, thus the effects from antecedent ST disappear in some cases. Both accumulated and concurrent variables can affect current ST by anomaly signal persistence and land-atmosphere interactions (Equation 19, Figures 7b and 7c); therefore, the existence of the signals similar to antecedent ST contained in the concurrent and accumulated influential variables can lead to the interactions between antecedent ST and current one. The signals similar to antecedent ST in concurrent variables arise from the high correlation between antecedent atmospheric forcing signals and current ones, such as concurrent SR (Figure 10). The signals similar to antecedent ST in accumulated variables arise from the high correlation between antecedent atmospheric forcing and the atmospheric forcing signals accumulated from antecedent to current time. In detail, when there are positive/negative correlations between influential variables and antecedent ST, and positive/negative correlations between influential variables and current ST, accumulated and concurrent influential variables enhance the lead-lag correlations between STs; while the influential variables make the lead-lag correlations between STs weaker in other conditions (Figure 8).

In some cases, antecedent ST is the most important factor in the lead-lag correlations between STs by the persistence of antecedent ST anomalies (Figure 5). However, in most cases, the signals from atmosphere play major roles in lead-lag correlations between STs, such as concurrent and accumulated net solar radiations. And these signals from atmosphere should be attributable either to the persistent forcing on atmosphere by land or ocean, or to similarities in antecedent and current forcing on atmosphere by land or ocean due to the shorter memory of atmosphere dynamic and thermodynamic processes relative to land and ocean. In other words, the atmosphere is only the medium through which land or ocean influences the relationships between antecedent and current STs in the above cases.

The relationships between the variables in current time and the ones in future time play crucial role in climate prediction. At the monthly, seasonal and longer time scales, the relationships between atmospheric variables at different time lags generally depend on sea surface temperature, soil moisture, ST, snow cover, sea ice etc. due to their longer memory relative to atmospheric variables. Therefore, on time scales longer than 1 month, the lead-lag correlations between near-surface temperatures may be related to the variables with long memory. Previous researches on the lead-lag relationships between near-surface air temperatures mainly focused on the persistence of air temperature anomalies, using methods including autocorrelation (Leasor et al., 2019), fractional integration (Lenti & Gil-Alana, 2021), the detrended fluctuation analysis (Capparelli et al., 2011), etc. However, these studies mainly analyzed the characteristics of temperature persistence, and lacked the analysis of corresponding influential factors and physical processes. Furthermore, there are even fewer studies on the physical mechanism of the lead-lag relationships between near-surface air temperatures. This study puts forward a new idea of studying the lead-lag correlations between air temperatures, and conducts preliminary research on the associated influential factors and possible physical processes, which have rarely been mentioned before. In addition, the deviations between reanalysis data and the corresponding observation data may affect the reliability of the conclusions using the above method, and the increase in influencing factors requires longer data for analysis. Nonetheless, this method combined with corresponding physical equations can be used to explain the correlations between variables in the climate system, helping to understand complex interactions in the climate system.

Data Availability Statement

The monthly station data in this manuscript is from the China National Stations' Fundamental Elements Datasets V3.0 (National Meteorological Information Center, 2019), which can be obtained from: http://data.tpdc.ac.cn/en/data/52c77e9c-df4a-4e27-8e97-d363fdfce10a/. ERA5 reanalysis data is from https://cds.climate.copernicus.eu/cdsapp#!/search?type=dataset%26text=ERA5 (Hersbach et al., 2020).

Acknowledgments

This work was supported by the National Natural Science Foundation of China (Grants 42130609, 41975081, and 41005047), the CAS "Light of West China" Program (E12903010, Y929641001), the Jiangsu University "Blue Project" outstanding young teachers training object, the Fundamental Research Funds for the Central Universities and the Jiangsu Collaborative Innovation Center for Climate Change.

References

Alexander, L. V., Zhang, X., Peterson, T. C., Caesar, J., Gleason, B., Klein Tank, A. M., et al. (2006). Global observed changes in daily climate extremes of temperature and precipitation. *Journal of Geophysical Research*, *111*(D5), D05109. https://doi.org/10.1029/2005JD006290

Capparelli, V., Vecchio, A., & Carbone, V. (2011). Long-range persistence of temperature records induced by long-term climatic phenomena. *Physical Review E*, *84*(4), 046103. https://doi.org/10.1103/PhysRevE.84.046103

Fang, S., Qi, Y., Yu, W., Liang, H., Han, G., Li, Q., et al. (2017). Change in temperature extremes and its correlation with mean temperature in mainland China from 1960 to 2015. *International Journal of Climatology*, *37*(10), 3910–3918. https://doi.org/10.1002/joc.4965

Gil-Alaña, L. A., Gupta, R., Sauci, L., & Carmona-González, N. (2022). Temperature and precipitation in the US states: Long memory, persistence, and time trend. *Theoretical and Applied Climatology*, *150*(3–4), 1731–1744. https://doi.org/10.1007/s00704-022-04232-z

He, J., Zhou, B., Wen, M., & Li, F. (2001). Vertical circulation structure, interannual variation features and variation mechanism of western Pacific subtropical high. *Advances in Atmospheric Sciences*, *18*(4), 497–510. https://doi.org/10.1007/s00376-001-0040-2

Hersbach, H., Bell, B., Berrisford, P., Hirahara, S., Horányi, A., Sabater, J., et al. (2020). The ERA5 global reanalysis [Dataset]. Quarterly Journal of the Royal Meteorological Society, *146*(730), 1999–2049. https://doi.org/10.1002/qj.3803

Holton, J. R. (2004). *Introduction to dynamic meteorology* (4th ed.). Elsevier, Academic Press.

IPCC. (2012). *Managing the risks of extreme events and disasters to advance climate change adaptation*. Cambridge University Press.

Kolstad, E. W., Barnes, E. A., & Sobolowski, S. P. (2017). Quantifying the role of land–atmosphere feedbacks in mediating near-surface temperature persistence. *Quarterly Journal of the Royal Meteorological Society*, *143*(704), 1620–1631. https://doi.org/10.1002/qj.3033

Kolstad, E. W., Sobolowski, S. P., & Scaife, A. A. (2015). Intraseasonal persistence of European surface temperatures. *Journal of Climate*, *28*(13), 5365–5374. https://doi.org/10.1175/JCLI-D-15-0053.1

Leasor, Z. T., Quiring, S. M., Ford, T. W., & McRoberts, D. B. (2019). Spatiotemporal variations in temperature persistence in the south-central United States. *Climate Research*, *77*(2), 181–192. https://doi.org/10.3354/cr01550

Lenti, J., & Gil-Alana, L. A. (2021). Time trends and persistence in European temperature anomalies. *International Journal of Climatology*, *41*(9), 4619–4636. https://doi.org/10.1002/joc.7090

Li, J., Sun, Z., & Zhang, F. (2021). Accounting for the surface temperature persistence by using signal energy. *Theoretical and Applied Climatology*, *144*(1–2), 363–377. https://doi.org/10.1007/s00704-020-03493-w

Lin, Z., Zuo, Z., Zhang, R., Xiao, D., You, Q., & Qiao, L. (2022). Persistence of soil enthalpy drives the winter and summer climate connection in the Tibetan Plateau. *Geophysical Research Letters*, *49*(12), e2022GL098503. https://doi.org/10.1029/2022GL098503

Lorenz, E. N. (1969). Three approaches to atmospheric predictability. *Bulletin of the American Meteorological Society*, *50*(5), 345–349. https://doi.org/10.1175/1520-0477-50.5.345

Mariotti, A., Ruti, P. M., & Rixen, M. (2018). Progress in subseasonal to seasonal prediction through a joint weather and climate community effort. *NPJ Climate and Atmospheric Science*, *1*(1), 4. https://doi.org/10.1038/s41612-018-0014-z

Matsumura, S., & Yamazaki, K. (2012). A longer climate memory carried by soil freeze–thaw processes in Siberia. *Environmental Research Letters*, *7*(4), 045402. https://doi.org/10.1088/1748-9326/7/4/045402

Nan, S., & Li, J. (2003). The relationship between the summer precipitation in the Yangtze River valley and the boreal spring Southern Hemisphere annular mode. *Geophysical Research Letters*, *30*(24), 2266. https://doi.org/10.1029/2003gl018381

National Meteorological Information Center. (2019). Daily meteorological dataset of basic meteorological elements of China National Surface Weather Station (V3.0) [Dataset]. National Tibetan Plateau Data Center. Retrieved from http://data.tpdc.ac.cn/en/data/52c77e9c-df4a-4e27-8e97-d363fdfce10a/

Oleson, K., Lawrence, D. M., Bonan, G. B., Drewniak, B., Huang, M., Koven, C. D., et al. (2013). *Technical description of version 4.5 of the community Land model (CLM)*. *NCAR Technical Note NCAR/TN-503+STR* (p. 434). National Center for Atmospheric Research.

Rypdal, K., Østvand, L., & Rypdal, M. (2013). Long-range memory in Earth's surface temperature on time scales from months to centuries. *Journal of Geophysical Research: Atmospheres*, *118*(13), 7046–7062. https://doi.org/10.1002/jgrd.50399

Schaefer, K. M., Zhang, T., Tans, P. P., & Stöckli, R. (2007). Temperature anomaly reemergence in seasonally frozen soils. *Journal of Geophysical Research*, *112*(D20), D20102. https://doi.org/10.1029/2007JD008630

Song, Y., Huang, A., & Chen, H. (2022a). The persistence and reemergence of atmospheric anomaly signals in soil temperature. *Journal of Geophysical Research: Atmospheres*, *127*(19), e2022JD037218. https://doi.org/10.1029/2022JD037218

Song, Y., Huang, A., & Chen, H. (2022b). The storage of antecedent precipitation and air temperature signals in soil temperature over China. *Journal of Hydrometeorology*, *23*(3), 377–388. https://doi.org/10.1175/JHM-D-21.0126.1

Wang, B., & Xu, X. (1997). Northern Hemisphere summer monsoon singularities and climatological intraseasonal oscillation. *Journal of Climate*, *10*(5), 1071–1085. https://doi.org/10.1175/1520-0442(1997)010<1071:NHSMSA>2.0.CO;2

Xie, J., Yu, J., Chen, H., & Hsu, P. C. (2020). Sources of subseasonal prediction skill for heatwaves over the Yangtze River basin revealed from three S2S models. *Advances in Atmospheric Sciences*, *37*(12), 1435–1450. https://doi.org/10.1007/s00376-020-0144-1

Yang, K., & Zhang, J. (2016). Spatiotemporal characteristics of soil temperature memory in China from observation. *Theoretical and Applied Climatology*, *126*(3–4), 739–749. https://doi.org/10.1007/s00704-015-1613-9

Zhan, Y., & Lin, Z. (2011). The relationship between June precipitation over mid-lower reaches of the Yangtze River basin and spring soil moisture over the East Asian monsoon region. *Acta Meteorologica Sinica*, *25*(3), 355–363. https://doi.org/10.1007/s13351-011-0310-6

Zhou, J., Zuo, Z., & Rong, X. (2020). Comparison of the effects of soil moisture and El Niño on summer precipitation in eastern China. *Science China Earth Sciences*, *63*(2), 267–278. https://doi.org/10.1007/s11430-018-9469-6

Zhou, J., Zuo, Z., Rong, X., & Wen, J. (2020). Role of May surface temperature over eastern China in East Asian summer monsoon circulation and precipitation. *International Journal of Climatology*, *40*(15), 6396–6409. https://doi.org/10.1002/joc.6588

Zong, H. F., Cholaw, B., Chen, L. T., Ren, J. L. R., & Wei, J. (2012). A typical mode of seasonal circulation transition: A climatic view of the abrupt transition from drought to flood over the middle and lower reaches of the Yangtze River Valley in the late spring and early summer of 2011. *Atmospheric and Oceanic Science Letters*, *5*(5), 349–354. https://doi.org/10.1080/16742834.2012.11447018

Zong, Y., & Chen, X. (2000). The 1998 flood on the Yangtze, China. *Natural Hazards*, *22*(2), 165–184. https://doi.org/10.1023/A:1008119805106